Chemosphere 303 (2022) 134917

Contents lists available at ScienceDirect

Chemosphere

journal homepage: www.elsevier.com/locate/chemosphere

Highly efficient poly(acrylic acid-*co*-aniline) grafted itaconic acid hydrogel: Application in water retention and adsorption of rhodamine B dye for a sustainable environment

Sourbh Thakur [a,b,**], Jyoti Chaudhary [b], Abhishek Thakur [c], Oguzhan Gunduz [d], Walaa F. Alsanie [e], Charalampos Makatsoris [f], Vijay Kumar Thakur [g,h,*]

[a] Department of Organic Chemistry, Bioorganic Chemistry and Biotechnology, Silesian University of Technology, B. Krzywoustego 4, 44-100, Gliwice, Poland
[b] School of Advanced Chemical Sciences, Shoolini University, Solan, 173229, Himachal Pradesh, India
[c] Department of Physics, Gautam Group of Colleges, Hamirpur, 177001, Himachal Pradesh University, India
[d] Center for Nanotechnology & Biomaterials Application and Research, Marmara University, Istanbul, Turkey
[e] Department of Clinical Laboratories Sciences, The Faculty of Applied Medical Sciences, Taif University, P.O. Box 11099, Taif, 21944, Saudi Arabia
[f] Department of Engineering, Faculty of Natural, Mathematical & Engineering Sciences, King's College London, United Kingdom
[g] Biorefining and Advanced Materials Research Center, Scotland's Rural College (SRUC), Edinburgh, EH9 3JG, United Kingdom
[h] School of Engineering, University of Petroleum and Energy Studies (UPES), Dehradun, 248007, India

HIGHLIGHTS

- Poly(acrylic acid-*co*-aniline) grafted itaconic acid (ItA-g-poly(AA-*co*-ANi) hydrogel has been synthesized.
- ItA-g-poly(AA-*co*-ANi) hydrogel showed maximum swelling of 1755.3%.
- ItA-g-poly(AA-*co*-ANi) hydrogel demonstrated high rhodamine b dye adsorption tendency of 925.9 mg g^{-1}.
- ItA-g-poly(AA-*co*-ANi) hydrogel exhibited significant soil-water retention properties.

ARTICLE INFO

Handling Editor: Govarthanan Muthusamy

Keywords:
Itaconic acid
Hydrogel
Swelling
Rhodamine B dye
Adsorption
Water retention

ABSTRACT

The present study used a free radical co-polymerization approach to synthesize a smart hydrogel of itaconic acid grafted poly(acrylic acid-*co*-aniline) (ItA-*g*-poly(AA-*co*-ANi)). ItA-g-poly(AA-*co*-ANi) hydrogel was characterized by Fourier transform infrared spectroscopy (FT-IR), Raman, X-ray diffraction (XRD), thermogravimetric analysis (TGA), field emission scanning electron microscope (FE-SEM), and X-ray photoelectron spectroscopy (XPS) analysis. Rhodamine B (RhB) dye was removed from an aqueous medium using ItA-g-poly(AA-*co*-ANi) hydrogel. To determine the maximum adsorption, the effect of parameters such as initial dye concentration, contact time, pH, and adsorbent dose were examined. The ItA-g-poly(AA-*co*-ANi) hydrogel had a high swelling percentage of 1755.3%. The high water penetration of ItA-g-poly(AA-*co*-ANi) hydrogel with a high swelling rate exposed the internal adsorption sites for RhB dye adsorption. The adsorption performance of ItA-g-poly(AA-*co*-ANi) hydrogel was explained by the pseudo-first-order and Freundlich adsorption isotherm models. Moreover, after four adsorption-desorption cycles, the ItA-g-poly(AA-*co*-ANi) hydrogel maintained an adsorption efficiency of 85.2%. The high water retention ability of ItA-g-poly(AA-*co*-ANi) hydrogel improved the moisture maintenance limit of soil for irrigation up to 23 days. As a result, ItA-g-poly(AA-*co*-ANi) hydrogel can be used in the elimination of toxic dyes as well as in irrigation systems.

* Corresponding author. Biorefining and Advanced Materials Research Center, Scotland's Rural College (SRUC), Edinburgh, EH9 3JG, United Kingdom.
** Corresponding author. Department of Organic Chemistry, Bioorganic Chemistry and Biotechnology, Silesian University of Technology, B. Krzywoustego 4, 44-100, Gliwice, Poland..
E-mail addresses: Sourbh.Thakur@polsl.pl, thakursourbh@gmail.com (S. Thakur), harris.makatsoris@kcl.ac.uk (C. Makatsoris), vijay.thakur@sruc.ac.uk (V.K. Thakur).

https://doi.org/10.1016/j.chemosphere.2022.134917
Received 19 November 2021; Received in revised form 18 April 2022; Accepted 7 May 2022
Available online 12 May 2022

1. Introduction

Nowadays, polluted wastewater count as one of the biggest problems worldwide (Ashvinder K. Rana et al., 2021a, 2021b; Ashvinder Kumar Rana et al., 2021; Thakur and Thakur, 2014). In modern times, dyes are broadly utilized in industries like textile, such as temporary hair coloring and paper coloring. The existence of toxic dye in water resources from these industries is the cause of wastewater (Lu et al., 2010). However, in the environment, the existence of dye contaminates water to a great extent creates the major cause of environmental problems. It can lead to many health issues, such as eye irritation, skin allergies, jaundice, and tissue necrosis (Kumar et al., 2005; Thakur and Voicu, 2016). Hence, effluent dye treatment is essential for a healthy lifestyle. Among distinct techniques, adsorption has been paid significant attention as a favorable technique due to some benefits, for example, low operation cost, excellent removal efficiency, high regeneration, and reusability chance (Sharma et al., 2020; Thakur et al., 2022; Thakur and Arotiba, 2018a; Thakur and Thakur, 2015; Verma et al., 2020).

Various dyes have been effectively adsorbed through several different adsorbents, including metal oxides, activated carbons, clays, and polymers. The above-mentioned adsorbents have a few shortcomings, for example, poor adsorption capability, lack of specificity, poor separation and regeneration ability (El-Salamony et al., 2017; Shandilya et al., 2018). The development of hydrogel as an adsorbent material has significant attention for adsorption of contaminants from aquatic media because of various advantages, including hydrophilic nature, bio-compatibility, and renewability (Ates et al., 2020; Chaudhary et al., 2021; Gautam et al., 2020; Thakur et al., 2018; Thakur and Arotiba, 2018a).

Hydrogels are water insoluble but sweallable in nature, having three dimensional polymeric networks that attract significant attention as a functional polymer and possess excellent water or fluid absorption capacity (Ning et al., 2021). Hydrogels are known as smart material due to its versatile and biocompatible characteristic. The specific structure networks of hydrogels show their compatibility towards various conditions for use. Due to the absorption ability of water content, hydrogel present their flexible behaviour which makes it feasible to perform in different conditions ranging from industrial to biological parameters (Thakur et al., 2019).

Water scarcity is one of the major biggest problems faced worldwide. Scarcity of water makes tough challenges against the food production from agricultural land, while researchers have been investigated the alternative against water scarcity for agriculture land. Hydrogels can be utilized as water retaining agents in regeneration of arid and dry land (Chaudhary et al., 2020; Pragna et al., 2017). Hydrogels can help to reduce water irrigation demand, increase fertilizer retention characteristics in soil, lowering plant death rates, and result in an extraordinary improvement in plant development due to excellent water absorption and retention performance (El-Hendawy and Schmidhalter, 2010; Mohawesh, 2015).

The creation of cross-linked hydrogel materials using conducting materials like aniline (ANi) has been paid significant attention in recent years, and facile technique can offers to combine the excellent properties of ANi in excellently crosslinked materials (Liu et al., 2012). Polyaniline is classified as a bifunctional polymer due to the inclusion of functional amine and imine groups, which function as a suitable backbone to remove the hazardous dye molecules from polluted water (Jain et al., 2017).

Itaconic acid (ItA) is a monomer (unsaturated) acid that contains two ionizable groups that allow to form hydrogen bonding (Kirimura et al., 1997). Generally, ItA extracted from renewable feedstocks and is similar to carbohydrate resources such as hydrolyzed starch (Zambanini et al., 2017). Because of their natural sources, ItA-based hydrogels are eco-friendly, hydrophilic, and capable of demonstrating lower toxicity (Sirviö et al., 2021). A little quantity of itaconic acid monomer can enhance the nature of imbibing characteristic of hydrogels (Yu et al., 2011). Moreover, itaconic acid can shows excellent absorption properties in polymer chemistry, environmental chemistry, pharmaceutical, drug delivery, and agriculture purposes (Shou et al., 2021). Related to itaconic acid grafted poly(acrylic acid-*co*-aniline) hydrogel study has not been reported.

In this research work, an initiative was taken to prepare itaconic acid grafted poly(acrylic acid-*co*-aniline) (ItA-*g*-poly(AA-*co*-ANi)) hydrogel via free radical copolymerization method. The percentage swelling was evaluated with respect to distinct reaction parameters including pH, reaction time, temperature variations, solvent amount, the concentration of monomer, initiator, and crosslinker. The smart ItA-g-poly(AA-*co*-ANi) hydrogel has been described on the basis of morphological analysis, thermal stability, functional group estimation, crystalline/amorphous character and elemental estimation via FE-SEM, TGA, FT-IR and Raman, XRD, and XPS analysis, respectively. The synthesized smart ItA-g-poly(AA-*co*-ANi) hydrogel has been examined for the adsorption of RhB dye. In addition, the crosslinked smart ItA-g-poly(AA-*co*-ANi) hydrogel water retention performance was tested in a soil sample to ensure application in an arid field. These samples have been preferred for their environmental interest and farming value. The synthesized ItA-g-poly(AA-*co*-ANi) hydrogel has excellent dye adsorption property and absorbs a huge amount of water and maintains the soil water moisture for irrigation purposes.

2. Experimental

2.1. Materials and reagents

Itaconic acid ($C_5H_6O_4$, 99%) (ItA), acrylic acid ($C_3H_4O_2$, 98%) (AA), aniline ($C_6H_5NH_2$, 99.5%) (ANi), potassium persulfate ($K_2S_2O_8$, 98%) (KPS) and N,N′-methylene bis-acrylamide ($C_7H_{10}N_2O_2$, 99%) (MBA), sodium hydroxide (NaOH, 45%) and hydrochloric acid (HCl, 37%), all chemicals were bought from Loba Chemie, India. Rhodamine B ($C_{28}H_{31}N_2O_3Cl$, 80%) (RhB) was bought from Central Drug House (CDH), India.

2.2. Instrumentation

On an Agilent technologies L1600312 FTIR spectrophotometer, the KBr pellet method was employed to analyze FTIR spectra in the spectrum band of 4000 to 400 cm^{-1}. Raman spectra of prepared ItA-g-poly (AA-*co*-ANi) hydrogel were analyzed via Lab RAM HR evolution Raman spectrophotometer. XRD spectral interpretation was acquired using a Smartlab 9 kW Rigaku corporation X-ray beam diffractometer with a scanning scaling range of $2\theta = 10–80^{\circ}$ and a probing rate of 2° min^{-1}. XPS spectra were investigated on a Nexsa base Thermo fisher scientific surface analyzer. The EXSTAR TGA 6300 thermogravimetric analyzer was used for the TGA analysis with a heating rate of 10 °C min^{-1}. JFEI (Nova- Nano SEM-450) FE-SEM was utilized to evaluate the morphological interpretations. The UV–Visible spectra of all adsorption parameter factors were analyzed using a Wensar LMSP-UV1900 spectrophotometer.

2.3. Preparation of ItA-g-poly(AA-co-ANi)) hydrogel

Scheme 1 depicts the general synthesis of ItA-g-poly(AA-*co*-ANi) hydrogel. Firstly, 1 g of itaconic acid was dissolved in 5 mL of deionized water. Additionally, AA (3.5×10^{-2} mol L^{-1}), ANi (0.3×10^{-2} mol L^{-1}), and KPS (0.09 mol L^{-1}) were added to this solution, followed with further insertion of MBA (0.12 mol L^{-1}) and was stirred for 30 min at room temperature. Then, 45 min of free radical polymerization at 70 °C had been carried out. The transparent insoluble colloidal gel has been attributed to the of ItA-g-poly(AA-*co*-Ani) hydrogel formation. ItA-g-poly(AA-*co*-ANi) hydrogel has been washed several times with the help of acetone and deionized water (Liu et al., 2012) to remove the unreacted monomers. ItA-g-poly(AA-*co*-ANi) hydrogel was dried in the

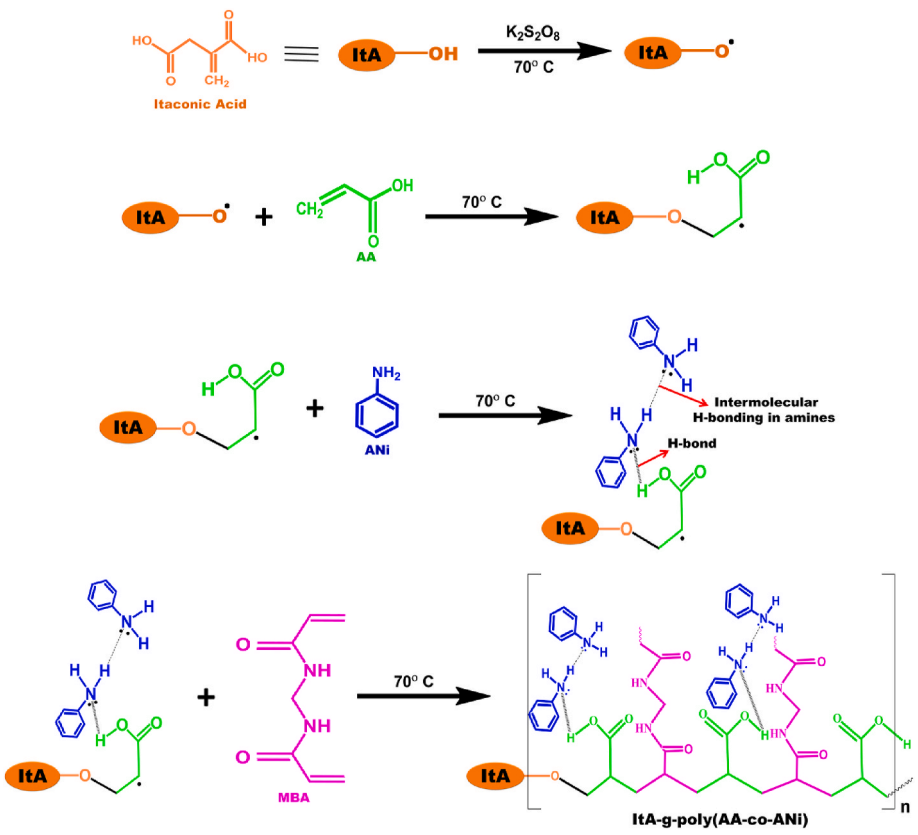

Scheme 1. Possible mechanism for synthesis of ItA-g-poly(AA-*co*-ANi) hydrogel.

oven at 50 °C until attained a consistent weight. By varying the amounts of ItA, AA, and ANi, a series of ItA-g-poly(AA-*co*-ANi) hydrogels were formed. A number of reaction parameters (reaction contact period, temperature variation, solvent volume, pH, variation in quantity of monomer, initiator, and cross-linker) were performed to optimize the ItA-g-poly(AA-*co*-ANi) hydrogel with superior water-absorbing ability.

2.4. Swelling studies of ItA-g-poly(AA-co-ANi) hydrogels

The pre-weighted ItA-g-poly(AA-*co*-ANi) hydrogel was placed in deionized water and kept at room temperature for 18 h without any disturbance. The swollen ItA-g-poly(AA-*co*-ANi) hydrogel was drained for a short time until no extra water remained. An analytical weighing balance was used to weigh the swelled ItA-g-poly(AA-*co*-ANi) hydrogel. The maximum swelling percentage was evaluated through equation (1) as:

$$\%\ \text{Swelling} = \frac{W_s - W_d}{W_d} \times 100 \tag{1}$$

W_s denotes the weight of the swelled ItA-g-poly(AA-*co*-ANi) hydrogel, while W_d denotes the weight of dried ItA-g-poly(AA-*co*-ANi) hydrogel.

2.5. Adsorption studies of RhB dye

Batch RhB adsorption analysis on ItA-g-poly(AA-*co*-ANi) hydrogel was performed via UV–visible spectroscope. Different adsorption parameters, for example, dose of ItA-g-poly(AA-*co*-ANi) hydrogel, pH, contact time, and temperature were analyzed to achieve ideal adsorption conditions. Spectrophotometric analysis was carried out through UV–Visible spectra with the help of a double-beam spectrophotometer at 525 nm, deionized water was utilized as reference solvent. For a specific RhB adsorption, 30 mg of ItA-g-poly(AA-*co*-ANi) hydrogel dose was used in 30 mL RhB dye (50 ppm solution) for 90 min. The solution was shaken at 200 rpm on a thermostatic shaker. Equation (2) was used to compute the maximum adsorption efficiency (Thakur and Arotiba, 2018a).

$$\text{Adsorption efficiency} = \frac{C_0 - C_t}{C_0} \times 100 \tag{2}$$

where C_0 stands for the initial absorbance and C_t presents the absorbance of RhB after time t.

2.6. Reusability study

Adsorption-desorption analysis was used to determine the recyclability of ItA-g-poly(AA-*co*-ANi) hydrogel. The RhB adsorbed ItA-g-poly (AA-*co*-ANi) hydrogel was regenerated and reused by cleaning through 0.05 M solution of HCl, after that neutralized through 0.05 M solution of NaOH. Collected ItA-g-poly(AA-*co*-ANi) adsorbent was again rinsed via deionized water and dried at room temperature (25 °C). After that, ItA-g-poly(AA-*co*-ANi) hydrogel was again used for the adsorption of RhB.

2.7. Water-retention study of ItA-g-poly(AA-co-ANi) hydrogel

The ItA-g-poly(AA-*co*-ANi) hydrogel water preservation analysis was performed in soil collected from Shoolini University, Solan, Himachal Pradesh, India. 20 g soil and 2 g ItA-g-poly(AA-*co*-ANi) hydrogel were homogenized in a plastic container, 30 mL water was added gradually, and the weight (W_1) was determined using a weighing machine. The container was weighed every day (W_2) and kept at room temperature until there was no consistency in weight loss. The water loss ratio (W %) of soil samples was calculated through standard formula (Hasija et al., 2018; Wu et al., 2008) as:

$$W\ \% = \frac{(W_1 - W_2)}{30} \times 100 \tag{3}$$

The experiments without ItA-g-poly(AA-*co*-ANi) hydrogel was also performed.

3. Results and discussion

3.1. Mechanism of ItA-g-poly(AA-co-ANi) hydrogel formation

ItA-g-poly(AA-*co*-ANi) hydrogel was formed using the co-polymerization method, and Scheme 1 shows the possible mechanism of the ItA-g-poly(AA-*co*-ANi) hydrogel network. Temperature utilized in co-polymerization created the reactive sites on monomers and led to the propagation of polymerization. KPS was a thermal initiator, and when it decomposed at high temperatures, it formed sulphate ion radicals and initiated the co-polymerization of acrylic acid and aniline to produce the network chain of poly(AA-*co*-ANi). On polar –OH units of itaconic acid, free radicals were induced. The monomer molecules in immediate contact with the active sites became acceptors of itaconic acid radicals, resulting in chain initiation, and the molecules around them then became free radical donors (Bao et al., 2011; Pourjavadi et al., 2007). The vinyl units of crosslinking agents could react with polymer network during chain propagation to develop ItA-g-poly(AA-*co*-ANi) hydrogel network.

3.2. Optimization of ItA-g-poly(AA-co-ANi) hydrogel swelling

3.2.1. Initiator

The impact of KPS (initiator) concentration on percentage swelling of ItA-g-poly(AA-*co*-ANi) hydrogel was examined by varying the KPS from 0.05 mol L^{-1} to 0.12 mol L^{-1} (Fig. 1a). Swelling percentage was improved initially with increasing the KPS concentration up to 0.09 mol L^{-1}, beyond 0.09 mol L^{-1}, percent swelling started decreasing. Maximum percent swelling (893.6%) was observed at 0.09 mol L^{-1}. The increase in percent swelling at low initiator concentration (<0.09 mol L-1) was ascribed to an adequate number of available active free radicals for copolymerization. At higher concentration (>0.09 mol L^{-1}), extreme production of free radicals directed to the early termination of the reactions, promoted the homopolymerization reaction, hence, low swelling (Saber-Samandari et al., 2012).

3.2.2. Reaction time

Various reaction time (35–55 min) was used to synthesized the ItA-g-poly(AA-*co*-ANi) hydrogel. Swelling percentage was enhanced from 825.5% to 906.6% for 35 min to 45 min respectively (Fig. 1b). The lessening of the all consumed reactants might be responsible for the decrease in % swelling during longer reaction times (>45 min) (Sharma et al., 2021).

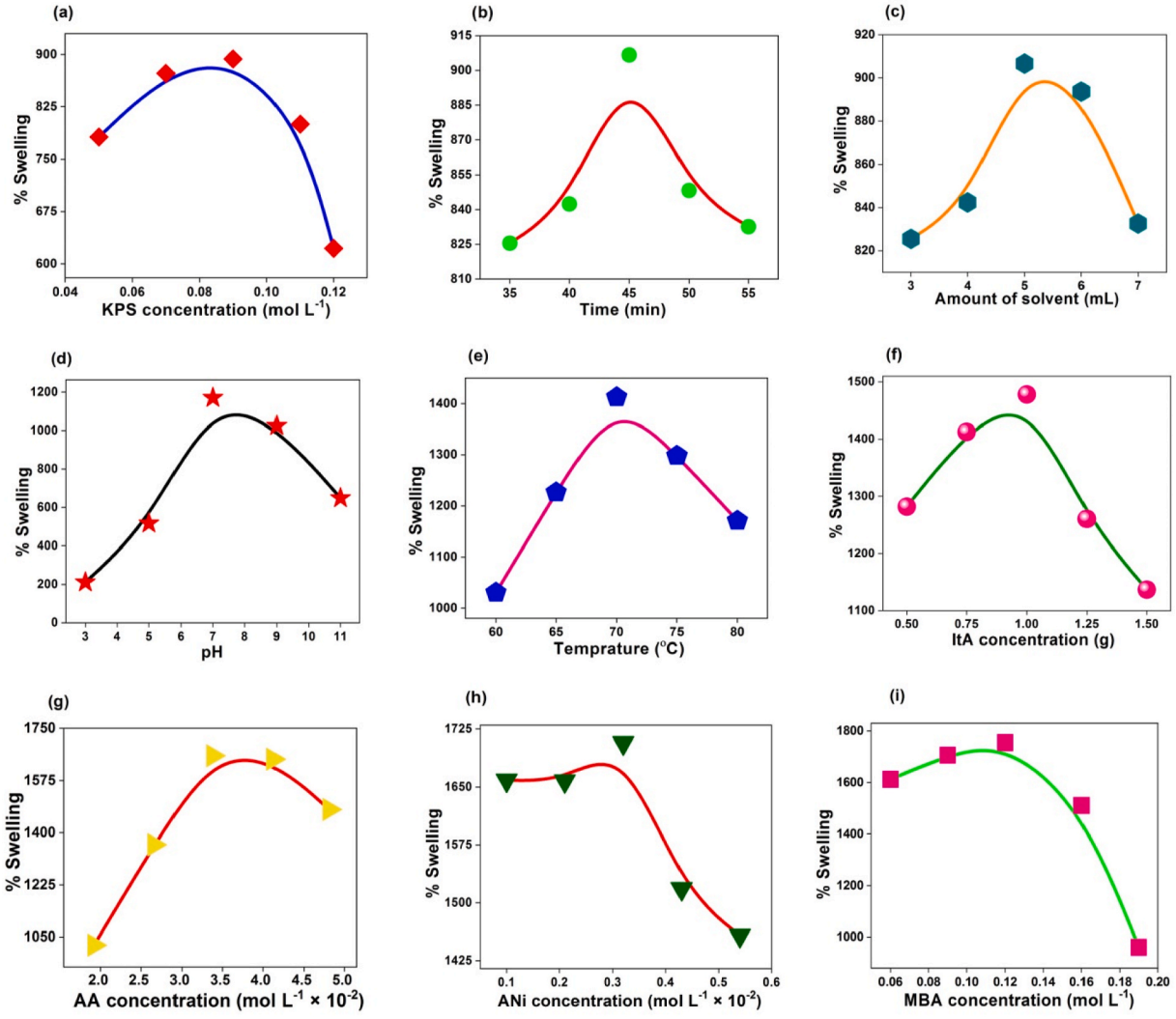

Fig. 1. ItA-g-poly(AA-*co*-ANi) hydrogel swelling percentage variation as a function of **(a)** KPS concentration, **(b)** time period, **(c)** solvent amount, **(d)** pH, **(e)** temperatures, **(f)** ItA concentration, **(g)** AA concentration, **(h)** ANi concentration, and **(i)** MBA concentration.

3.2.3. Solvent

Fig. 1c demonstrates the impact of solvent (H_2O) volume onto swelling percentage of ItA-g-poly(AA-*co*-ANi) hydrogel. The swelling percentage was firstly increased up to 5 mL of solvent and then decreased from 5 mL to 7 mL. Hydroxyl radicals produced from H_2O (solvent) helped in propagation of copolymerization reaction resulted improvement in swelling percentage. The increase in solvent volume (>5 mL) led to dilution and reduced the swelling percentage (Pourjavadi et al., 2008).

3.2.4. pH

pH had a significant impact on the swelling ability of ItA-g-poly(AA-*co*-ANi) hydrogel. In the pH range of 3–11, the effect of pH on ItA-g-poly (AA-*co*-ANi) hydrogel swelling was examined (Fig. 1d). The maximum swelling percentage was obtained at neutral pH, ItA-g-poly(AA-*co*-ANi) hydrogel swelling was reduced at either high or low pH. The protonation of COO^- groups at low pH led to a decrease in electrostatic repulsions, the 3D structure of the ItA-g-poly(AA-*co*-ANi) hydrogel matrix got collapsed, hence low swelling. The charge density was balanced at neutral pH, leading to high ItA-g-poly(AA-*co*-ANi) swelling. Under the basic condition, carboxylic groups were ionised into COO^- and excess of COO^- caused the collapse of the 3D structure of ItA-g-poly(AA-*co*-ANi) hydrogel, resulted in low swelling (Rezanejade Bardajee et al., 2008).

3.2.5. Temperature

ItA-g-poly(AA-*co*-ANi) hydrogel swelling percentage was enhanced from 60 °C to 70 °C, and maximum swelling percentage (1412.5%) was obtained at 70 °C (Fig. 1e). KPS was effectively decomposed at higher temperatures, and increased temperature promoted the activation of free radicals, which was ascribed to improved ItA-g-poly(AA-*co*-ANi) hydrogel swelling. The more active free radicals were effectively enhanced the copolymerization and grafting reactions (Thakur and Arotiba, 2018b), hence, formed ItA-g-poly(AA-*co*-ANi) hydrogel could absorb more water. At temperatures beyond 70 °C, excessive cross-linking occurred, resulting in a more compact and stiff structure, leading to reduced swelling (Zhang et al., 2007).

3.2.6. Itaconic acid

ItA-g-poly(AA-*co*-ANi) hydrogel swelling percentage was highest at the ItA amount of 1.0 g (Fig. 1f). Increasing the ItA amount from 0.50 g to 1.0 g makes more ItA molecules available for the chain propagation sites on graft copolymer network, attributed to enhanced ItA-g-poly(AA-*co*-ANi) hydrogel swelling percentage. ItA amount higher than 1.0 g led to increase the rate of homopolymerization reaction and a decrease in ItA-g-poly(AA-*co*-ANi) swelling percentage (Chen and Zhao, 2000).

3.2.7. Acrylic acid

The swelling behaviour of ItA-g-poly(AA-*co*-ANi) hydrogel was studied at various AA concentrations varying from 2.1×10^{-2} mol L^{-1} to 5.0×10^{-2} mol L^{-1}. As shown in Fig. 1g, ItA-g-poly(AA-*co*-ANi) hydrogel swelling percentage, increased with AA concentration, and reached maximum (1658.8%) at 3.5×10^{-2} mol L^{-1}. This was probably because of the superior accessibility of AA molecules. The decrease in ItA-g-poly(AA-*co*-ANi) hydrogel swelling percentage at higher AA concentration (>3.5×10^{-2} mol L^{-1}) was assigned to the development of self-crosslinking, which enhanced the viscosity of the reaction mixture and hindered free radical movement (Mishra et al., 2011). Similar outcomes have been recorded previously (Saber-Samandari et al., 2012).

3.2.8. Aniline

Various ANi concentrations (0.1×10^{-2} mol L^{-1} to 0.6×10^{-2} mol L^{-1}) were examined for ItA-g-poly(AA-*co*-ANi) hydrogel swelling (Fig. 1h). At 0.3×10^{-2} mol L^{-1}, the highest ItA-g-poly(AA-*co*-ANi) hydrogel swelling (1707%) was achieved, however, as the ANi concentration was increased beyond 0.3×10^{-2} mol L^{-1}, the ItA-g-poly(AA-*co*-ANi) swelling percentage was decreased. It might be due to the compactness and hydrophobic property of ANi (Tang et al., 2008).

3.2.9. Crosslinker

Crosslinker inhibits hydrophilic polymer networks from dissolving in the aqueous phase and effectively makes the hydrogel insoluble. According to Flory's network theory, for controlling crosslinking density and fluid absorbency, the presence of crosslinking chains is essential (Cheng et al., 2013). ItA-g-poly(AA-*co*-ANi) hydrogel swelling studies were carried out at different crosslinker (MBA) concentrations varying from 0.06 mol L^{-1} to 0.19 mol L^{-1} (Fig. 1i). The grafted ItA-g-poly (AA-*co*-ANi) copolymer showed maximum swelling of 1755.3% at 0.12 mol L^{-1}. For crosslinker concentrations of more than 0.12 mol L^{-1}, ItA-g-poly(AA-*co*-ANi) hydrogel swelling started to reduce. It could be because the ItA-g-poly(AA-*co*-ANi) hydrogel network developed a significant number of cross-linked chains, resulted stiff structure (Sharma et al., 2021).

3.3. Characterization

3.3.1. FTIR

FTIR spectroscopy confirmed the structural difference between ItA, ItA-g-poly(AA-*co*-ANi) hydrogel, and RhB adsorbed ItA-*g*-poly(AA-*co*-ANi) hydrogel (Fig. 2). The broad peaks at 3031 cm^{-1} in the ItA spectrum corresponded to –OH stretching, 2923.5 cm^{-1} was assigned to $-CH_2$ asymmetric stretching mode (Kumar et al., 2013), the peak of C–C bending vibration occurred at 1413.5 cm^{-1} (Miloudi et al., 2017). The C═O stretching vibration was assigned at 1681.6 cm^{-1}, while the C–O–C stretching vibration was assigned a peak at 1189.8 cm^{-1} (Rani et al., 2012). After graft copolymerization of AA/ANi on ItA, a sharp and intense peak at 1704.7 cm^{-1} corresponded to the C═O bond of carboxylic acid (Fan et al., 2008). The peak at 1423.2 cm^{-1} was induced by AA, attributed to the symmetric stretching mode of –COO. The carboxylate group's stretching vibration led to a new peak at 1164.7 cm^{-1} (Makhado et al., 2018). Fig. 2b presents the FTIR of RhB adsorbed ItA-g-poly(AA-*co*-ANi) hydrogel, N–H stretching bond of 2° amine of RhB was found at 3730.2 cm^{-1}. In addition, the aromatic C–N bonding was confirmed at 1402.4 cm^{-1} and the –OH stretching aromatic ring bond was found at 1156.5 cm^{-1}, which were characteristics of RhB dye. Because of the adsorption of RhB dye on ItA-g-poly(AA-*co*-ANi) hydrogel, the stretching vibration of the C–H bond was changed from 2933.1 cm^{-1} to 2930.1 cm^{-1}. The sharp N–H peaks have been relocated from 1423 cm^{-1} to 1402.4 cm^{-1} and 1704 cm^{-1} to 1628.9 cm^{-1} after adsorption of the RhB (Singh et al., 2017).

3.3.2. Raman analysis

The Raman spectral interpretation of ItA, ItA-g-poly(AA-*co*-ANi) hydrogel, and RhB adsorbed ItA-*g*-poly(AA-*co*-ANi) hydrogel are shown in Fig. 3. The out-of-plane bending of $=CH_2$ corresponded to the peak at 729.5 cm^{-1}, 1655.4 cm^{-1} for stretching mode of C═O, and peak nearly around 2936.4 cm^{-1} corresponded to the asymmetric stretching vibration mode of the $-CH_2$ (Yang and Gu, 2001). In Raman spectrum of ItA-g-poly(AA-*co*-ANi) hydrogel, the peak appeared around 1092.4 cm^{-1} for C–CH_2 stretching, 1708.1 cm^{-1} for C═O stretching, and 2937.5 cm^{-1} for stretching of CH_2 or CH group (Dong et al., 1997; Klement et al., 2021), the appearance of these peaks showed the presence of AA/ANi in the hydrogel network. Moreover, the shifting of the peak from 729.5 cm^{-1} to 568.8 cm^{-1} might be due to the grafting of AA/ANi onto ItA. RhB adsorbed ItA-g-poly(AA-*co*-ANi) hydrogel showed the appearance of a broad peak hump at 2085.7 cm^{-1}.

3.3.3. XRD analysis

XRD patterns of ItA and ItA-g-poly(AA-*co*-ANi) hydrogel are described in the 2θ range of 5°–90° (Fig. 4a). ItA spectra showed fundamental diffraction peaks at 19.5°, 26.2°, 30.4°, 34.5°, 48.1°, and 52.3° corresponded to (111), (220), (311), (400), (511), and (440), respectively (Parthiban et al., 2020), which demonstrated the crystalline

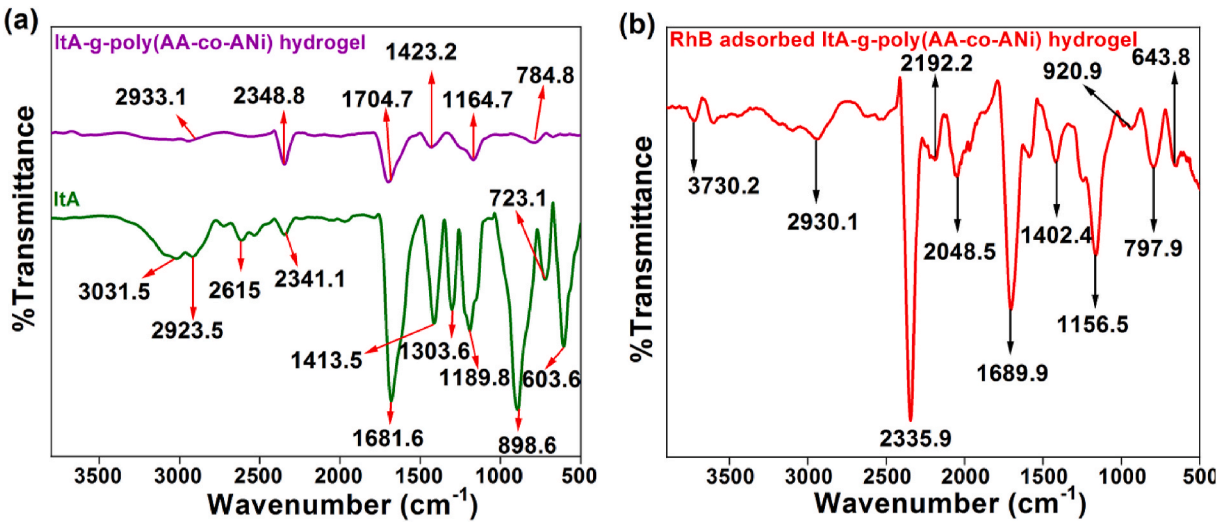

Fig. 2. FT-IR spectra of **(a)** ItA, ItA-g-poly(AA-*co*-ANi) hydrogel and **(b)** RhB adsorbed ItA-g-poly(AA-*co*-ANi) hydrogel.

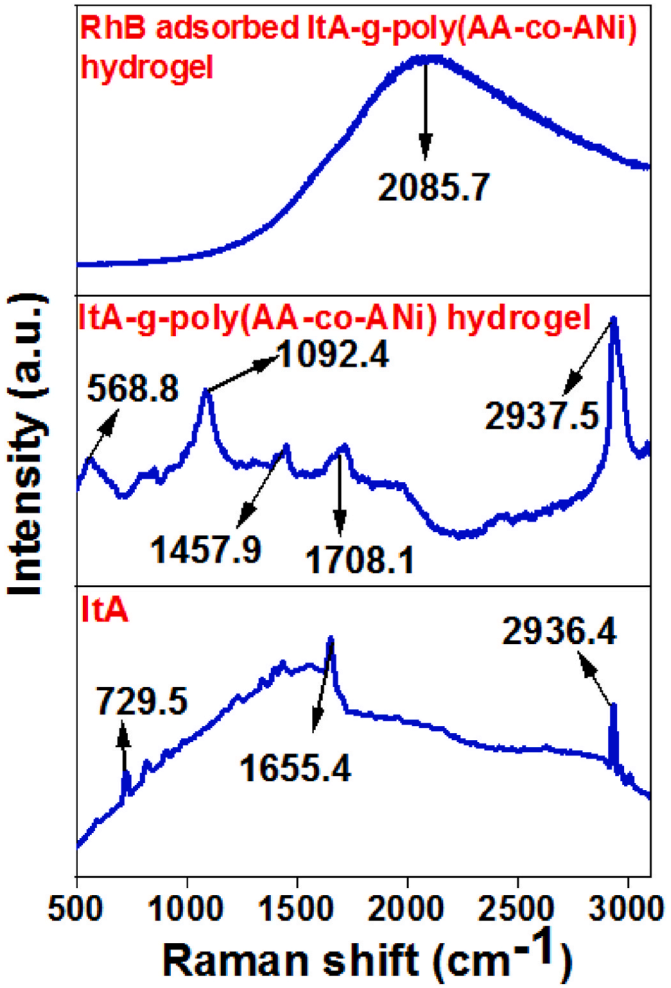

Fig. 3. Raman spectra of ItA, ItA-g-poly(AA-*co*-ANi) hydrogel and RhB adsorbed ItA-*g*-poly(AA-*co*-ANi) hydrogel.

characteristic of ItA. The grafting of AA/Ani on itaconic acid showed major transformation in the XRD pattern of ItA-g-poly(AA-*co*-ANi) hydrogel. The hydroxyl groups of ItA were affected by AA/ANi, which destroyed the crystalline structure and transformed it to amorphous.

3.3.4. TGA analysis

TGA analysis of ItA-g-poly(AA-*co*-ANi) hydrogel has been introduced in Fig. 4b. The weight loss in ItA-g-poly(AA-*co*-ANi) hydrogel happened through three-stage decomposition. From 23 °C to 100 °C, the ItA-g-poly (AA-*co*-ANi) hydrogel lost 4% of weight, which could be related to the loss of entrapped water molecules in the gel network. The second observable degradation of the ItA-g-poly(AA-*co*-ANi) hydrogel was found in the range of 165 °C–275 °C, which was recognized for the loss of carbonyl group, NH group, and COOH group (Mbese and Ajibade, 2014). Around 90% weight loss was observed in sharp loss during the third step in the range of 275 °C–548 °C. Dehydration of the polymeric network, depolymerization of copolymer chains, and hydrogel network disintegration into minute molecules of carbon were all part for the last step of degradation (Maity and Ray, 2017; Reddy et al., 2013). Further heating over 548 °C resulted in no weight loss.

3.3.5. XPS analysis

XPS is employed to attain complete information regarding the chemical composition of the synthesized ItA-g-poly(AA-*co*-ANi) hydrogel (Fig. 5a–d). The full scan spectrum of ItA-g-poly(AA-*co*-ANi) hydrogel (Fig. 5a) specified the existence of O, N, and C, signified hydrogel's purity. Fig. 5b shows the high-resolution spectral interpretation of O 1s, which showed two significant peaks at 532.6 eV and 534.08 eV, which were due to the C═O and C–O bonds, respectively. The occurrence of N-atoms as the R–NH_2 group was confirmed by two peaks in the high resolution spectral interpretation of N 1s, observed at around 392.08 eV and 397.7 eV (Fig. 5c). Meanwhile, the three most prominent peaks in the C 1s XPS interpretation (Fig. 5d) were observed at 289.4 eV, 286.7 eV, and 285.4 eV, which were caused by O–C═O, C–O–C, and C–C bonds, respectively (Shandilya et al., 2018).

3.3.6. SEM analysis

The surface morphology of ItA, ItA-g-poly(AA-*co*-ANi) hydrogel, and RhB adsorbed ItA-*g*-poly(AA-*co*-ANi) hydrogel are shown in Fig. 6. Fig. 6a demonstrates the morphology of ItA, which presented big rock like shape with a gradually smooth surface. In comparison to smooth ItA (Fig. 6a), ItA-g-poly(AA-*co*-ANi) hydrogel displayed a rough and porous surface (Fig. 6b). The porosity increased the surface area, which was advantageous for increasing the number of absorption sites per unit area with improved adsorption properties. The surface transition from itaconic acid to graft co-polymers was noticed, signifying the grafting of AA/ANi onto ItA. Fig. 6c demonstrated the occurrence of the RhB layer that covered the ItA-g-poly(AA-*co*-ANi) hydrogel surface because of the adsorption process.

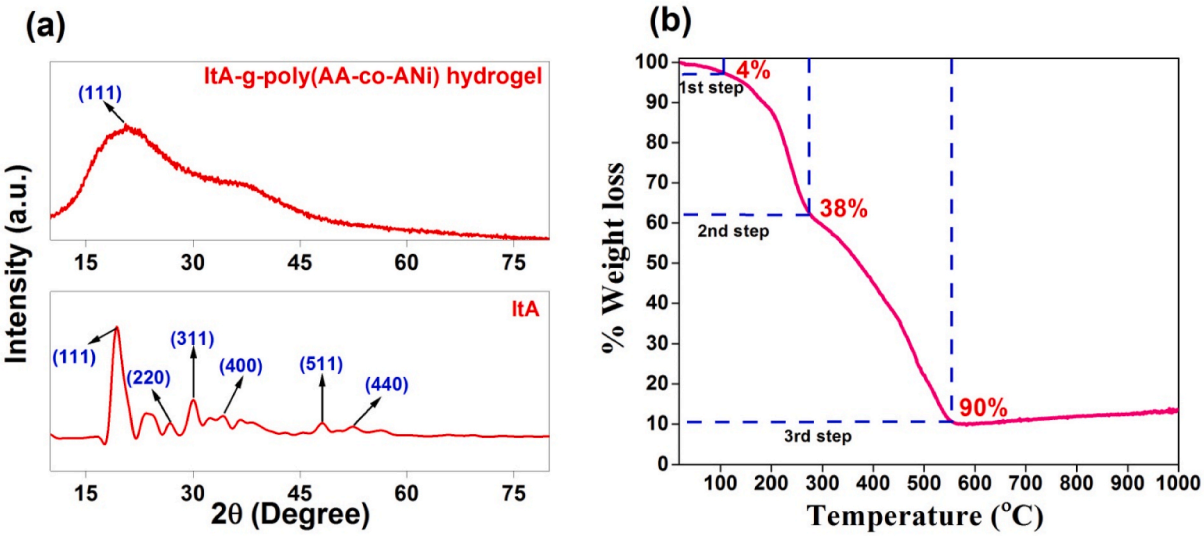

Fig. 4. XRD pattern of **(a)** ItA and ItA-g-poly(AA-*co*-ANi) hydrogel and TGA pattern for **(b)** ItA-g-poly(AA-*co*-ANi) hydrogel.

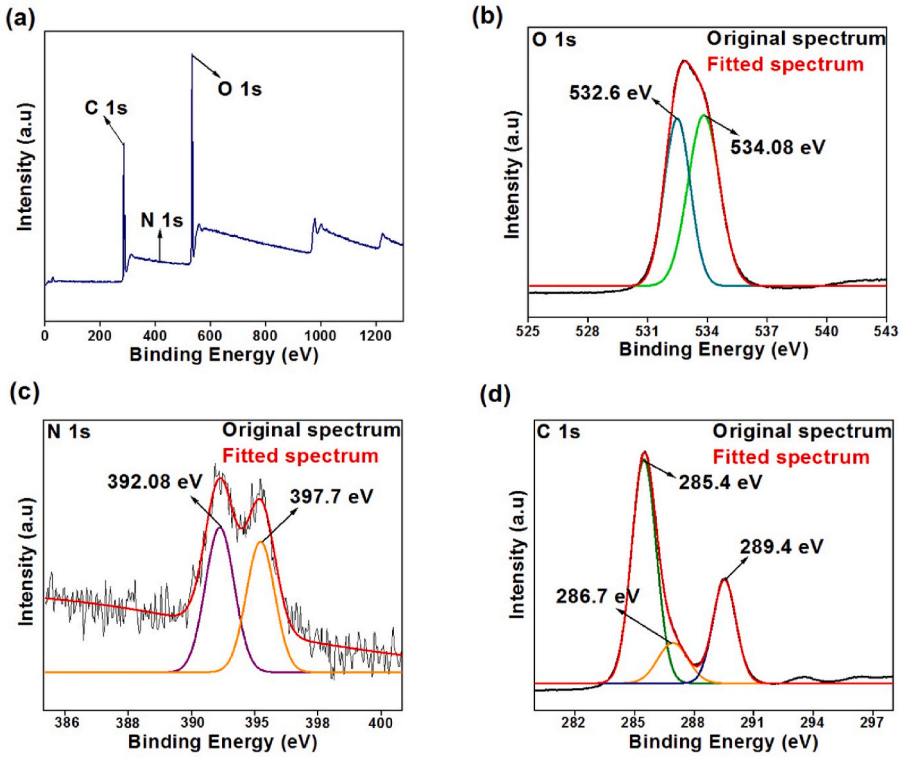

Fig. 5. XPS spectrum of **(a)** ItA-g-poly(AA-*co*-ANi) hydrogel and XPS high resolution interpretation of **(b)** O 1s, **(c)** N 1s and **(d)** C 1s.

3.4. Adsorption of RhB onto ItA-g-poly(AA-co-ANi) hydrogel

3.4.1. Effect of pH

Batch adsorption experimental analyses were performed by changing the pH from 1 to 10 (Fig. 7a). The percentage removal of RhB was increased from 64.4% to 87.9%, with pH varied from 1 to 7, respectively. Moreover, at high pH, the observed percentage removal was slightly low, the percentage removal of RhB was 83.9% at pH 10. At low pH, the H^+ ions interacted with cationic dye molecules for binding sites in ItA-g-poly(AA-*co*-ANi) hydrogel, thus reducing dye adsorption performance (Parthiban et al., 2020). Due to electrostatic interactions among negatively charged ItA-g-poly(AA-*co*-ANi) hydrogel and positively charged dye, the maximum adsorption of dye was observed at pH 7 (87.9%) (Scheme 2). As a result, pH 7 was chosen as the optimal pH for continuing adsorption studies (Parthiban et al., 2020).

3.4.2. Adsorbent dose

The impact of ItA-g-poly(AA-*co*-ANi) adsorbent dose on RhB adsorption was examined in the range of 10–40 mg at pH 7 and RhB concentration of 50 ppm (Fig. 7b). The RhB removal percentage was increased from 37.5% to 87.9% for 10 mg to 30 mg respectively, and then became constant at above 30 mg. The availability of more adsorption active sites on ItA-g-poly(AA-*co*-ANi) adsorbent could explain the improvement in adsorption proficiency with increased

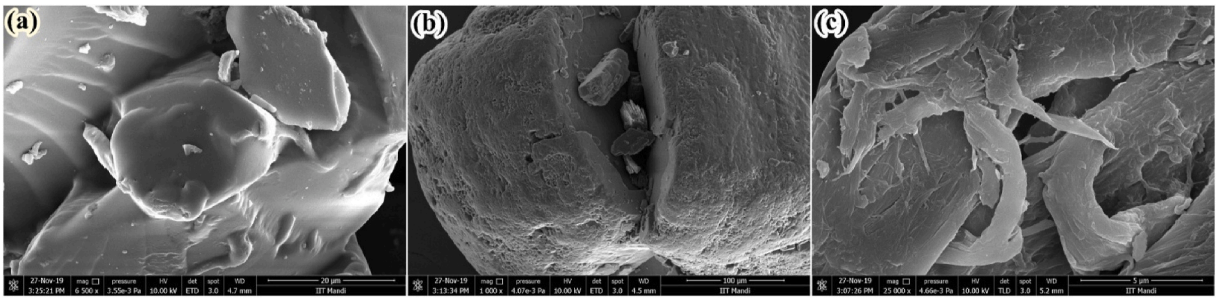

Fig. 6. SEM morphology of **(a)** ItA, **(b)** ItA-g-poly(AA-*co*-ANi) hydrogel and **(c)** RhB adsorbed ItA-*g*-poly(AA-*co*-ANi) hydrogel.

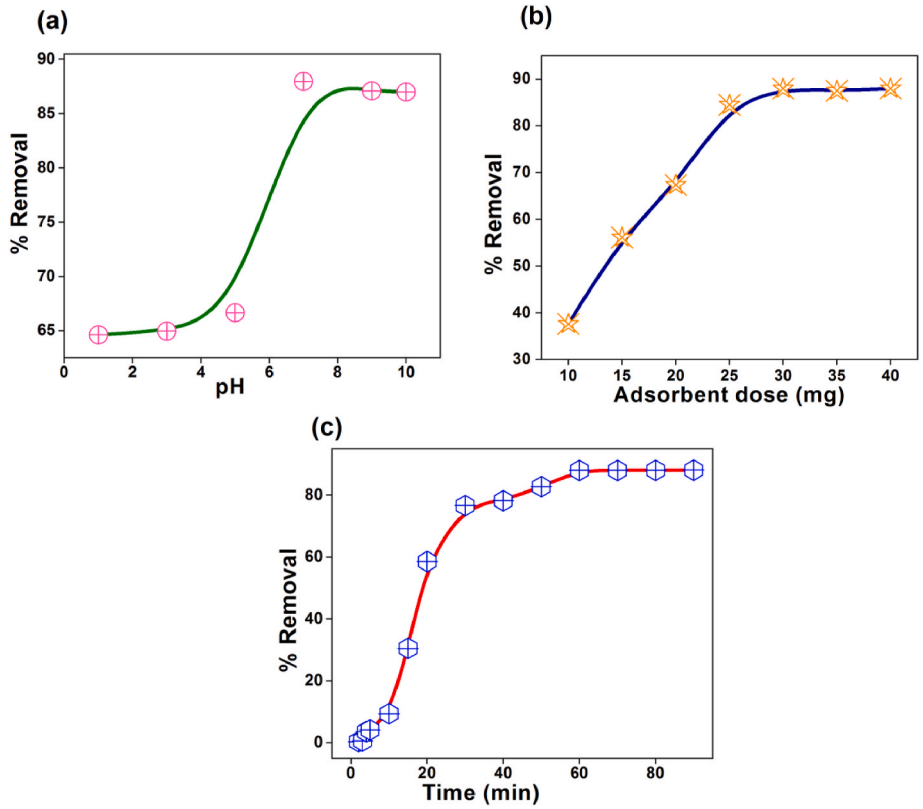

Fig. 7. Effect of **(a)** pH (adsorption parameters: RhB solution = 30 mL (50 mg L^{-1}), ItA-g-poly(AA-*co*-ANi) dose = 30 mg, pH = 7, time = 90 min at 25 °C), **(b)** adsorbent dose (adsorption parameters: pH = 7, RhB solution = 30 mL (50 mg L^{-1}), time = 90 min at 25 °C) and **(c)** time (adsorption parameters: pH = 7, RhB solution = 30 mL (50 mg L^{-1}), ItA-g-poly(AA-*co*-ANi) dose = 30 mg at 25 °C) on the removal of RhB dye using ItA-g-poly(AA-*co*-ANi) hydrogel.

adsorbent dose. Beyond the 30 mg adsorbent dose, the percent removal remained constant, this could be attributed to the greater competition among the different adsorbent, resulted a potential chemical split between the adsorbate and the adsorbent (Maity and Ray, 2017).

3.4.3. Contact time

The impact of time on the cationic dye (RhB) adsorption onto ItA-g-poly(AA-*co*-ANi) hydrogel was analyzed for contact time varies from 1 to 90 min at pH 7 (Fig. 7c). The percentage of RhB removal was increased rapidly with the contact time, with maximum RhB removal of 0.3% and 87.9% within 1 min and 60 min, respectively. The equilibrium was attained in 60 min, the maximum percentage adsorption was 87.9%. The initial increase might be attributed to increased contact possibilities between RhB molecules and the ItA-g-poly(AA-*co*-ANi) adsorbent, which finally led to equilibrium and the adsorption rate became leveled off.

3.5. Adsorption study

3.5.1. Adsorption kinetics

Fig. 8 demonstrates the RhB adsorption kinetic results, from which various kinetic model parameters (supplementary information) and rate constants were determined and thoroughly compared in Table S1. The R^2 values were compared to determine the most favorable kinetic model, and result revealed that the pseudo-first-order kinetic model (Fig. 8a) better clarified the RhB adsorption on ItA-g-poly(AA-*co*-ANi) as compared with the pseudo-second-order model (Fig. 8b) (Makhado et al., 2018). In addition, the intraparticle diffusion model was utilized for examining the adsorption information (Fig. 8c). This model can examines the absorption of dye molecules onto the ItA-g-poly(AA-*co*-ANi) hydrogel surface and pores.

3.5.2. Adsorption isotherms

The isotherm (supplementary information) investigation helps in the assurance of the type of adsorption. The values of various adsorption

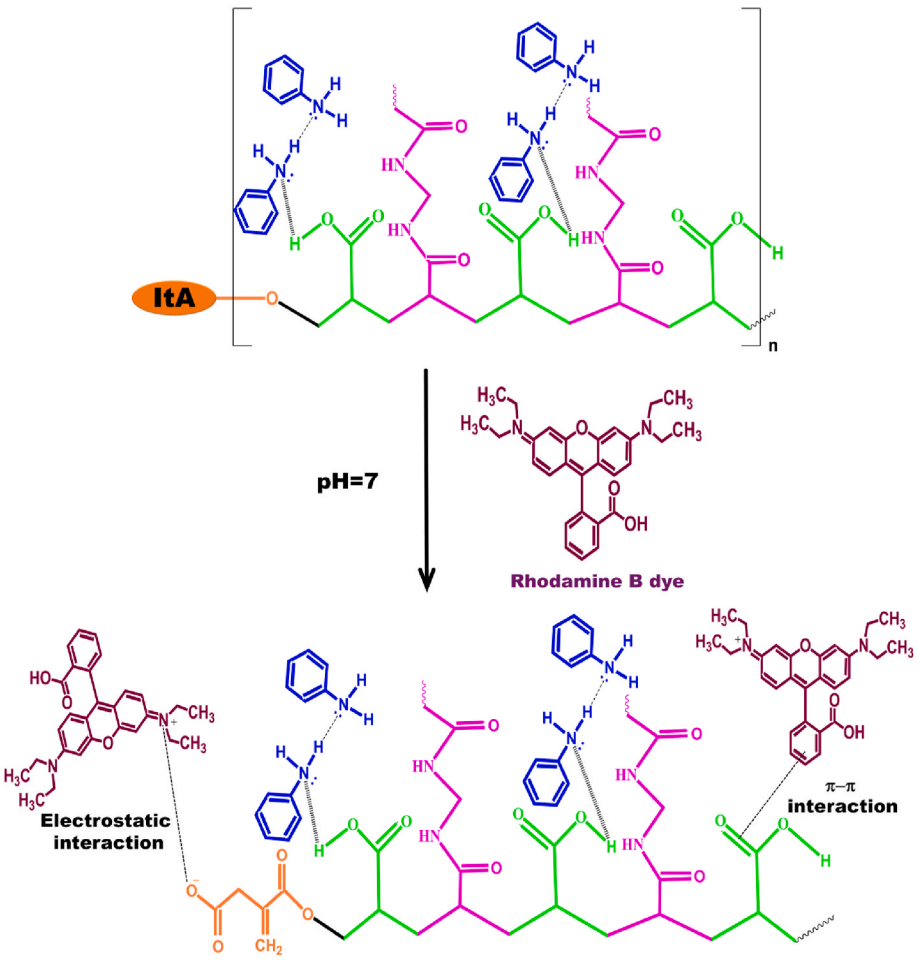

Scheme 2. Possible interaction scheme between RhB and ItA-g-poly(AA-*co*-ANi) hydrogel during adsorption.

variables and constants are listed in Table S2, and the linear fits are shown in Fig. 8d–f. Based on the regression coefficients (R^2) values, the Freundlich isotherm was best matched to the adsorption than the Langmuir and Temkin model. The maximum ItA-g-poly(AA-*co*-ANi) adsorption capacity (q_m) was determined as 925.92 mg g^{-1} at 25 °C.

3.6. Reusability

The reusability of ItA-g-poly(AA-*co*-ANi) hydrogel was examined through four adsorption-desorption cycles, and the results are shown in Figure S1. ItA-g-poly(AA-*co*-ANi) hydrogel demonstrated outstanding stability against RhB adsorption, with 87.9% at the first cycle, 87.3% at the second cycle, 86.9% at the third cycle, and 85.2% at the fourth successive adsorption-desorption cycles. This indicated the excellent adsorption capacity of fabricated ItA-g-poly(AA-*co*-ANi) hydrogel towards RhB removal and can be used as stable adsorbent for textile wastewater treatment.

3.7. Comparison of ItA-g-poly(AA-co-ANi) hydrogel performance with other adsorbents

Table S3 demonstrated that the synthesized ItA-g-poly(AA-*co*-ANi) hydrogel had a comparatively very high adsorption capacity than that of previously reported adsorbents. As natural toxic free inexpensive polymer, the occurrence of ItA, ANi, and AA forms biodegradable and eco-friendly hydrogel, offers significant functional group (–NH, –OH) units onto the surface of hydrogel, and make efficient RhB adsorption. Moreover, simple synthesis, ecological friendliness, high adsorption limit and stability factors make it a fascinating alternative for wastewater treatment.

3.8. Water retention properties of ItA-g-poly(AA-co-ANi) hydrogel

The water retention capabilities of synthesized ItA-g-poly(AA-*co*-ANi) hydrogel were investigated in soil experiments by recording the weight of the samples regularly until a consistent observation was acquired. Figure S2a-b shows the results of calculated water loss ratio in percentage. Water loss was lower in soil treated with ItA-g-poly(AA-*co*-ANi) hydrogel than in soil without ItA-*g*-poly(AA-*co*-ANi) hydrogel (control). As a result, the ItA-g-poly(AA-*co*-ANi) hydrogel can be utilized to transform arid regions into “fertile green regions” (Ghobashy et al., 2021). The moisture in the soil sample started to reduce as time passed (Figure S2a,b). However, the decrease rate was different for each soil sample with and without the ItA-g-poly(AA-*co*-ANi) hydrogels. The water loss ratio of the sandy loam soil without (control) and with ItA-g-poly(AA-*co*-ANi) hydrogels are presented in Figure S2a and Figure S2b, respectively. The sandy loam soil was mixed with the ItA-g-poly(AA-*co*-ANi) hydrogel demonstrated a slow water loss ratio. In pure sandy loam soil (control) system, within 10 days, the water retention ratio was reduced to 25%, while on the 11th day, the water retention ratio was reached to 0% (Figure S2c). In sandy loam soil with ItA-g-poly(AA-*co*-ANi) hydrogel, water retention ratio was 149% on 1st day, and the water retention ratio was approached to 107% in 18 days, instant decrease in water retention ratio was observed on 21st day, reduced to 58% and the similar trend of instant decrease in moisture retention ratio was observed at 22nd and 23rd day, water retention ratio

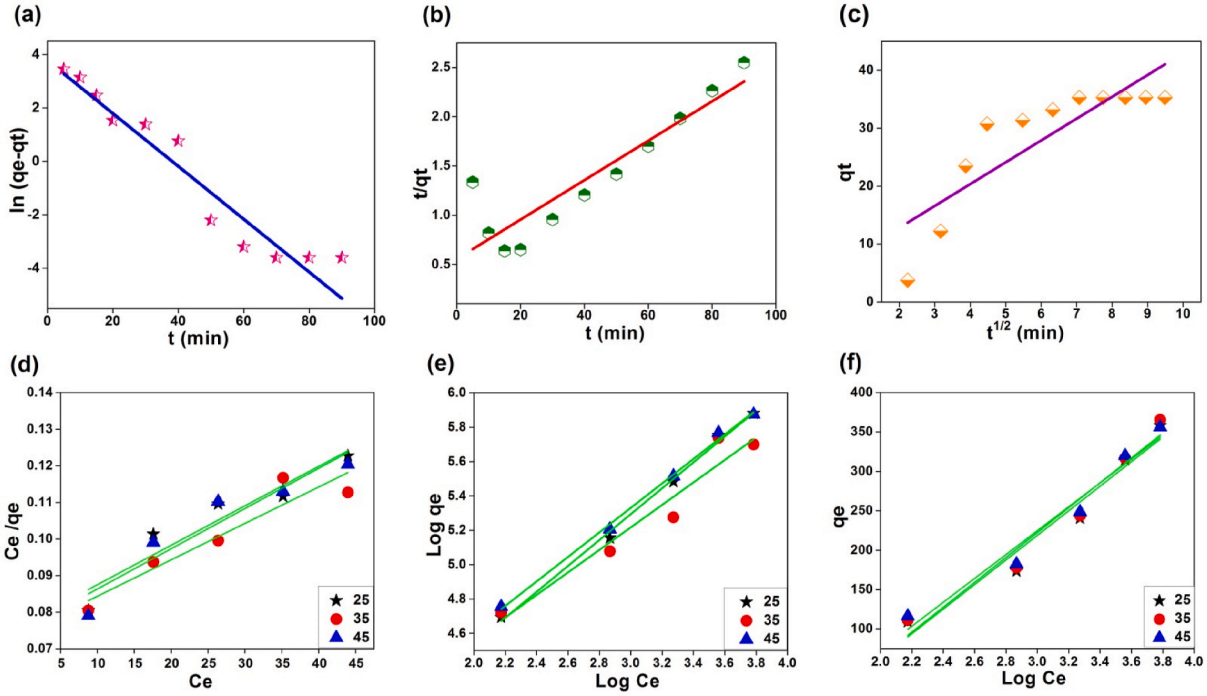

Fig. 8. Adsorption kinetic and isotherm adsorption models for RhB adsorption onto ItA-g-poly(AA-*co*-ANi) hydrogel: **(a)** pseudo-first-order, **(b)** pseudo-second-order, **(c)** intra-particle diffusion, (adsorption parameters: pH = 7, RhB solution = 30 mL (50 mg L^{-1}), ItA-g-poly(AA-*co*-ANi) dose = 30 mg, rpm = 200) and **(d)** Langmuir isotherm, **(e)** Freundlich isotherm, **(f)** Temkin model (adsorption parameters: pH = 7, RhB concentration = 100–500 mg L^{-1}, RhB volume = 30 mL, ItA-g-poly(AA-*co*-ANi) dose = 30 mg, rpm = 200).

was approached to 20% on 23rd day. After that, on the 24th day, the water retention ratio was reached to 0% (Figure S2c). Therefore, sandy loam soil with ItA-g-poly(AA-*co*-ANi) hydrogel showed 2.3 times better water retention capacity than the control system. In this manner, the fabricated ItA-g-poly(AA-*co*-ANi) hydrogel can be utilized effectively as water-sparing material in the agro field (Chaudhary et al., 2020).

4. Conclusion

The graft copolymerization process was used to make a novel ItA-g-poly(AA-*co*-ANi) hydrogel that has been used for RhB dye adsorption and water moisture-retaining purposes. The optimized parameter of ItA-g-poly(AA-*co*-ANi) hydrogel (KPS = 0.09 mol L^{-1}, time = 45 min, solvent = 5 mL, pH = 7, temperature = 70 °C, ItA = 1.0 g, AA = 3.5×10^{-2} mol L^{-1}, ANi = 0.3×10^{-2} mol L^{-1}, MBA = 0.12 mol L^{-1}) presented the highest swelling tendency of 1755.3% in deionized water. The 87.9% was the highest reported RhB adsorption on ItA-g-poly(AA-*co*-ANi) hydrogel at optimized condition (30 mL of 50 mg L^{-1} RhB solution, ItA-g-poly(AA-*co*-ANi) dose = 30 mg, pH = 7, time = 60 min). The optimum adsorption efficiency was 925.92 mg g^{-1}, and RhB adsorption fitted better with the Freundlich isotherm and the pseudo 1st order model. Moreover, recyclability of ItA-g-poly(AA-*co*-ANi) hydrogel was performed, exhibited 85.2% RhB adsorption even after four successive adsorption-desorption cycles. The prepared ItA-g-poly(AA-*co*-ANi) hydrogel showed 2.3 times better soil-water retention results in sandy loam soil than control media. Hence, recyclable developed ItA-g-poly (AA-*co*-ANi) hydrogel indicates brilliant RhB dye adsorption and can be utilized as an excellent adsorbent in textile's wastewater. ItA-g-poly(AA-*co*-ANi) hydrogel can significantly improve the soil water retention ability, which opens their candidature as promising water holding materials in farming land.

Credit author statement

Sourbh Thakur; Abhishek Thakur; Oguzhan Gunduz: Conceptualization, Methodology, Writing - Original Draft, Investigation, Visualization, Data Curation. Sourbh Thakur; Jyoti Chaudhary; Walaa F. Alsanie; Charalampos Makatsoris: Formal analysis, Investigation, Data Curation, Writing - Original Draft. Sourbh Thakur; Vijay Kumar Thakur: Supervision, Writing - review & editing.

Declaration of competing interest

The authors declare that they have no known competing financial interests or personal relationships that could have appeared to influence the work reported in this paper.

Acknowledgment

Sourbh Thakur acknowledges the National Science Center, Poland (under the Miniature-5, Grant agreement 2021/05/X/ST5/01522) for financial support of the research. Walaa F. Alsanie would like to acknowledge Taif University TURSP program (TURSP-2020/53) for funding.

Appendix A. Supplementary data

Supplementary data to this article can be found online at https://doi.org/10.1016/j.chemosphere.2022.134917.

References

Ates, B., Koytepe, S., Ulu, A., Gurses, C., Thakur, V.K., 2020. Chemistry, structures, and advanced applications of nanocomposites from biorenewable resources. Chem. Rev. 120, 9304–9362. https://doi.org/10.1021/acs.chemrev.9b00553.

Bao, Y., Ma, J., Li, N., 2011. Synthesis and swelling behaviors of sodium carboxymethyl cellulose-g-poly (AA-co-AM-co-AMPS)/MMT superabsorbent hydrogel. Carbohydr. Polym. 84, 76–82.

Chaudhary, J., Thakur, S., Mamba, G., Prateek, Gupta, R.K., Thakur, V.K., 2021. Hydrogel of gelatin in the presence of graphite for the adsorption of dye: towards the concept for water purification. J. Environ. Chem. Eng. 9, 104762. https://doi.org/10.1016/j.jece.2020.104762.

Chaudhary, J., Thakur, S., Sharma, M., Gupta, V.K., Thakur, V.K., 2020. Development of biodegradable agar-agar/gelatin-based superabsorbent hydrogel as an efficient moisture-retaining agent. Biomolecules 10, 939.
Chen, J., Zhao, Y., 2000. Relationship between water absorbency and reaction conditions in aqueous solution polymerization of polyacrylate superabsorbents. J. Appl. Polym. Sci. 75, 808–814.
Cheng, Z., Li, J., Yan, J., Kang, L., Ru, X., Liu, M., 2013. Synthesis and properties of a novel superabsorbent polymer composite from microwave irradiated waste material cultured Auricularia auricula and poly (acrylic acid-co-acrylamide). J. Appl. Polym. Sci. 130, 3674–3681.
Dong, J., Ozaki, Y., Nakashima, K., 1997. Infrared, Raman, and near-infrared spectroscopic evidence for the coexistence of various hydrogen-bond forms in poly (acrylic acid). Macromolecules 30, 1111–1117.
El-Hendawy, S.E., Schmidhalter, U., 2010. Optimal coupling combinations between irrigation frequency and rate for drip-irrigated maize grown on sandy soil. Agric. Water Manag. 97, 439–448.
El-Salamony, R.A., Amdeha, E., Ghoneim, S.A., Badawy, N.A., Salem, K.M., Al-Sabagh, A. M., 2017. Titania modified activated carbon prepared from sugarcane bagasse: adsorption and photocatalytic degradation of methylene blue under visible light irradiation. Environ. Technol. 38, 3122–3136.
Fan, S., Tang, Q., Wu, J., Hu, D., Sun, H., Lin, J., 2008. Two-step synthesis of polyacrylamide/poly (vinyl alcohol)/polyacrylamide/graphite interpenetrating network hydrogel and its swelling, conducting and mechanical properties. J. Mater. Sci. 43, 5898–5904.
Gautam, D., Lal, S., Hooda, S., 2020. Adsorption of rhodamine 6G dye on binary system of nanoarchitectonics composite magnetic graphene oxide material. J. Nanosci. Nanotechnol. 20, 2939–2945.
Ghobashy, M.M., El-Damhougy, B.K., El-Wahab, H.A., Madani, M., Amin, M.A., Naser, A. E.M., Abdelhai, F., Nady, N., Meganid, A.S., Alkhursani, S.A., Alshangiti, D.M., 2021. Controlling radiation degradation of a CMC solution to optimize the swelling of acrylic acid hydrogel as water and fertilizer carriers. Polym. Adv. Technol. 32, 514–524. https://doi.org/10.1002/pat.5105.
Hasija, V., Sharma, K., Kumar, V., Sharma, S., Sharma, V., 2018. Green synthesis of agar/Gum Arabic based superabsorbent as an alternative for irrigation in agriculture. Vacuum 157, 458–464.
Jain, P., Varshney, S., Srivastava, S., 2017. Site-specific functionalization for chemical speciation of Cr (III) and Cr (VI) using polyaniline impregnated nanocellulose composite: equilibrium, kinetic, and thermodynamic modeling. Appl. Water Sci. 7, 1827–1839.
Kirimura, K., Sato, T., Nakanishi, N., Terada, M., Usami, S., 1997. Breeding of starch-utilizing and itaconic-acid-producing koji molds by interspecific protoplast fusion between Aspergillus terreus and Aspergillus usamii. Appl. Microbiol. Biotechnol. 47, 127–131.
Klement, T., Kockmann, N., Schwede, C., Röder, T., 2021. Kinetic measurement of acrylic acid polymerization at high concentrations under nearly isothermal conditions in a Pendula slug flow reactor. Ind. Eng. Chem. Res. 60, 4240–4250.
Kumar, K.V., Ramamurthi, V., Sivanesan, S., 2005. Modeling the mechanism involved during the sorption of methylene blue onto fly ash. J. Colloid Interface Sci. 284, 14–21.
Kumar, R., Sharma, K., Tiwary, K.P., Sen, G., 2013. Polymethacrylic acid grafted psyllium (Psy-g-PMA): a novel material for waste water treatment. Appl. Water Sci. 3, 285–291.
Liu, Y., Hu, J., Zhuang, X., Zhang, P., Wei, Y., Wang, X., Chen, X., 2012. Synthesis and characterization of novel biodegradable and electroactive hydrogel based on aniline oligomer and gelatin: synthesis and characterization of novel. Macromol. Biosci. 12, 241–250.
Lu, X., Liu, L., Liu, R., Chen, J., 2010. Textile wastewater reuse as an alternative water source for dyeing and finishing processes: a case study. Desalination 258, 229–232.
Maity, J., Ray, S.K., 2017. Competitive removal of Cu (II) and Cd (II) from water using a biocomposite hydrogel. J. Phys. Chem. B 121, 10988–11001.
Makhado, E., Pandey, S., Nomngongo, P.N., Ramontja, J., 2018. Preparation and characterization of xanthan gum-cl-poly (acrylic acid)/o-MWCNTs hydrogel nanocomposite as highly effective re-useable adsorbent for removal of methylene blue from aqueous solutions. J. Colloid Interface Sci. 513, 700–714.
Mbese, J.Z., Ajibade, P.A., 2014. Preparation and characterization of ZnS, CdS and - Google Scholar. Polymers 6, 2332–2344.
Miloudi, L., Bonnier, F., Bertrand, D., Byrne, H.J., Perse, X., Chourpa, I., Munnier, E., 2017. Quantitative analysis of curcumin-loaded alginate nanocarriers in hydrogels using Raman and attenuated total reflection infrared spectroscopy. Anal. Bioanal. Chem. 409, 4593–4605.
Mishra, M.M., Yadav, M., Mishra, D.K., Behari, K., 2011. Synthesis of graft copolymer (CmgOH-g-NVP) and study of physicochemical properties: characterization and application. Carbohydr. Polym. 83, 1749–1756.
Mohawesh, O., 2015. Field evaluation of deficit irrigation effects on tomato growth performance, water-use efficiency and control of parasitic nematode infection. S. Afr. J. Plant Soil 1, 8.
Ning, F., Zhang, J., Kang, M., Ma, C., Li, H., Qiu, Z., 2021. Hydroxyethyl cellulose hydrogel modified with tannic acid as methylene blue adsorbent. J. Appl. Polym. Sci. 138, 49880. https://doi.org/10.1002/app.49880.
Parthiban, E., Kalaivasan, N., Sudarsan, S., 2020. Dual responsive (pH and magnetic) nanocomposites based on Fe 3 O 4@ polyaniline/itaconic acid: synthesis, characterization and removal of toxic hexavalent chromium from tannery wastewater. J. Inorg. Organomet. Polym. Mater. 30, 4677–4690.
Pourjavadi, A., Barzegar, S., Zeidabadi, F., 2007. Synthesis and properties of biodegradable hydrogels of κ-carrageenan grafted acrylic acid-co-2-acrylamido-2-methylpropanesulfonic acid as candidates for drug delivery systems. React. Funct. Polym. 67, 644–654.
Pourjavadi, A., Soleyman, R., Barajee, G.R., 2008. Novel nanoporous superabsorbent hydrogel based on poly (acrylic acid) grafted onto salep: synthesis and swelling behavior. Starch Staerke 60, 467–475.
Pragna, G., Jyothi, M., Kunari, N., Rao, I.B., 2017. The effect of different soil amendment on irrigation frequency, crop yield, water use efficiency of spinach. Int. J. Appl. Biol. Pharmaceut. Technol. 8, 12–18.
Rana, Kumar, Ashvinder, Frollini, E., Thakur, V.K., 2021. Cellulose nanocrystals: pretreatments, preparation strategies, and surface functionalization. Int. J. Biol. Macromol. 182, 1554–1581. https://doi.org/10.1016/j.ijbiomac.2021.05.119.
Rana, Ashvinder K., Gupta, V.K., Saini, A.K., Voicu, S.I., Abdellattifaand, M.H., Thakur, V.K., 2021a. Water desalination using nanocelluloses/cellulose derivatives based membranes for sustainable future. Desalination 520, 115359. https://doi.org/10.1016/j.desal.2021.115359.
Rana, Ashvinder K., Mishra, Y.K., Gupta, V.K., Thakur, V.K., 2021b. Sustainable materials in the removal of pesticides from contaminated water: perspective on macro to nanoscale cellulose. Sci. Total Environ. 797, 149129. https://doi.org/10.1016/j.scitotenv.2021.149129.
Rani, P., Sen, G., Mishra, S., Jha, U., 2012. Microwave assisted synthesis of polyacrylamide grafted gum ghatti and its application as flocculant. Carbohydr. Polym. 89, 275–281.
Reddy, P.M.K., Mahammadunnisa, S.K., Ramaraju, B., Sreedhar, B., Subrahmanyam, C., 2013. Low-cost adsorbents from bio-waste for the removal of dyes from aqueous solution. Environ. Sci. Pollut. Control Ser. 20, 4111–4124.
Rezanejade Bardajee, G., Pourjavadi, A., Sheikh, N., Sadegh Amini-Fazl, M., 2008. Grafting of acrylamide onto kappa-carrageenan via γ-irradiation: optimization and swelling behavior. Radiat. Phys. Chem. 77, 131–137.
Saber-Samandari, S., Gazi, M., Yilmaz, E., 2012. UV-induced synthesis of chitosan-g-polyacrylamide semi-IPN superabsorbent hydrogels. Polym. Bull. 68, 1623–1639.
Shandilya, P., Mittal, D., Soni, M., Raizada, P., Hosseini-Bandegharaei, A., Saini, A.K., Singh, P., 2018. Fabrication of fluorine doped graphene and SmVO4 based dispersed and adsorptive photocatalyst for abatement of phenolic compounds from water and bacterial disinfection. J. Clean. Prod. 203, 386–399.
Sharma, B., Thakur, S., Mamba, G., Gupta, R.K., Gupta, V.K., Thakur, V.K., 2021. Titania modified gum tragacanth based hydrogel nanocomposite for water remediation. J. Environ. Chem. Eng. 9, 104608.
Sharma, B., Thakur, S., Trache, D., Yazdani Nezhad, H., Thakur, V.K., 2020. Microwave-Assisted rapid synthesis of reduced graphene oxide-based gum tragacanth hydrogel nanocomposite for heavy metal ions adsorption. Nanomaterials 10, 1616.
Shou, Y., Campbell, S.B., Lam, A., Lausch, A.J., Santerre, J.P., Radisic, M., Davenport Huyer, L., 2021. Toward renewable and functional biomedical polymers with tunable degradation rates based on itaconic acid and 1, 8-octanediol. ACS Appl. Polym. Mater. 3, 1943–1955.
Singh, R., Ahlawat, O.P., Rajor, A., 2017. Decolourization of textile dyes by ligninolytic fungi isolated from spent mushroom substrate. Bull. Env. Pharmacol. Life Sci 6, 53–66.
Sirviö, J.A., Kantola, A.M., Komulainen, S., Filonenko, S., 2021. Aqueous modification of chitosan with itaconic acid to produce strong oxygen barrier film. Biomacromolecules 22, 2119–2128.
Tang, Q., Wu, J., Lin, J., 2008. A multifunctional hydrogel with high conductivity, pH-responsive, thermo-responsive and release properties from polyacrylate/polyaniline hybrid. Carbohydr. Polym. 73, 315–321.
Thakur, S., Arotiba, O.A., 2018a. Synthesis, swelling and adsorption studies of a pH-responsive sodium alginate–poly(acrylic acid) superabsorbent hydrogel. Polym. Bull. 75, 4587–4606.
Thakur, S., Arotiba, O.A., 2018b. Synthesis, swelling and adsorption studies of a pH-responsive sodium alginate–poly (acrylic acid) superabsorbent hydrogel. Polym. Bull. 75, 4587–4606.
Thakur, S., Chaudhary, J., Kumar, V., Thakur, V.K., 2019. Progress in pectin based hydrogels for water purification: trends and challenges. J. Environ. Manag. 238, 210–223.
Thakur, S., Sharma, B., Thakur, A., Kumar Gupta, V., Alsanie, W.F., Makatsoris, C., Kumar Thakur, V., 2022. Synthesis and characterisation of zinc oxide modified biorenewable polysaccharides based sustainable hydrogel nanocomposite for Hg2+ ion removal: towards a circular bioeconomy. Bioresour. Technol. 348, 126708. https://doi.org/10.1016/j.biortech.2022.126708.
Thakur, S., Sharma, B., Verma, A., Chaudhary, J., Tamulevicius, S., Thakur, V.K., 2018. Recent progress in sodium alginate based sustainable hydrogels for environmental applications. J. Clean. Prod. 198, 143–159. https://doi.org/10.1016/j.jclepro.2018.06.259.
Thakur, V.K., Thakur, M.K., 2015. Recent advances in green hydrogels from lignin: a review. Int. J. Biol. Macromol. 72, 834–847. https://doi.org/10.1016/j.ijbiomac.2014.09.044.
Thakur, V.K., Thakur, M.K., 2014. Recent advances in graft copolymerization and applications of chitosan: a review. ACS Sustain. Chem. Eng. 2, 2637–2652. https://doi.org/10.1021/sc500634p.
Thakur, V.K., Voicu, S.I., 2016. Recent advances in cellulose and chitosan based membranes for water purification: a concise review. Carbohydr. Polym. 146, 148–165. https://doi.org/10.1016/j.carbpol.2016.03.030.
Verma, A., Thakur, S., Mamba, G., Gupta, R.K., Thakur, P., Thakur, V.K., 2020. Graphite modified sodium alginate hydrogel composite for efficient removal of malachite green dye. Int. J. Biol. Macromol. 148, 1130–1139.
Wu, L., Liu, M., Liang, R., 2008. Preparation and properties of a double-coated slow-release NPK compound fertilizer with superabsorbent and water-retention. Bioresour. Technol. 99, 547–554.

Yang, C.Q., Gu, X., 2001. Polymerization of maleic acid and itaconic acid studied by FT-Raman spectroscopy. J. Appl. Polym. Sci. 81, 223–228.
Yu, Y., Li, Y., Liu, L., Zhu, C., Xu, Y., 2011. Synthesis and characterization of pH-and thermoresponsive poly (N-isopropylacrylamide-co-itaconic acid) hydrogels crosslinked with N-maleyl chitosan. J. Polym. Res. 18, 283–291.
Zambanini, T., Tehrani, H.H., Geiser, E., Merker, D., Schleese, S., Krabbe, J., Buescher, J. M., Meurer, G., Wierckx, N., Blank, L.M., 2017. Efficient itaconic acid production from glycerol with Ustilago vetiveriae TZ1. Biotechnol. Biofuels 10, 131.
Zhang, J., Wang, L., Wang, A., 2007. Preparation and properties of chitosan-g-poly (acrylic acid)/montmorillonite superabsorbent nanocomposite via in situ intercalative polymerization. Ind. Eng. Chem. Res. 46, 2497–2502.